A model of ion track structure based on classical collision dynamics (radiobiology application)

1986 Phys. Med. Biol. 31 1201

(http://iopscience.iop.org/0031-9155/31/11/002)

Phys. Med. Biol., 1986, Vol. 31, No 11, 1201–1209. Printed in Great Britain

A model of ion track structure based on classical collision dynamics

Jürgen Kiefer and Hermann Straaten

Strahlenzentrum der Justus-Liebig-Universität Giessen, Leihgesterner Weg 217, Giessen, West Germany

Received 2 September 1985, in final form 1 April 1986

Abstract. The energy deposition in ion tracks as a function of radial distance is calculated on the basis of classical collision dynamics and using empirical range–energy relationships for electrons. The calculations show that the energy density (i.e. energy deposited per unit mass) varies according to an inverse-square function with distance from the track centre. The maximum extension, the 'penumbra radius', is a power function of the ion's kinetic energy divided by its mass. Comparison with experimental data demonstrates the applicability of the model for ion specific energies greater than 1 MeV u^{-1}.

1. Introduction

The quantitative interpretation of biological heavy-ion effects (for recent reviews see Blakely *et al* 1984, Kiefer 1985) requires a knowledge of the spatial distribution of energy deposited within tracks, commonly referred to as 'track structure'. The radial extension is particularly critical with very heavy, energetic ions since they may deposit high amounts of energy even at comparatively large distances from the track centre due to the high density of far-ranging δ electrons. There are a number of models available in the literature (Butts and Katz 1967, Fain *et al* 1974, Chatterjee and Schaefer 1976, Chatterjee *et al* 1973, Hansen and Olsen 1984) based on different assumptions and simplifications. They all agree that the energy deposited per mass element—termed 'energy density' in the following—varies essentially with $1/x^2$, x being the distance from the track centre. They differ in the actual value of the energy density and particularly in the maximum extension x_p, the so-called 'penumbra radius'. Monte Carlo simulations which were given for protons, deuterons and α particles (Zaider *et al* 1983, Wilson and Paretzke 1981, Brenner and Zaider 1984, Paretzke 1974, 1980) have not yet been published for heavier ions. Because of the discrepancies mentioned it is felt worthwhile to treat the problem on the basis of classical collision dynamics making use of established experimental energy–range relationships for electrons. The results of the calculations are compared with experimental data.

2. Theoretical treatment

The model is based on three assumptions:

(1) secondary electrons liberated by heavy-ion impact of the exposed medium are ejected according to classical collision dynamics ('classical' is used here to mean that quantum-mechanical considerations are neglected);

0031-9155/86/111201+09$02.50

(2) the energy distribution of secondary electrons follows the inverse-square law; and

(3) the electrons travel in straight lines, their range being related to their kinetic energy by a simple power function.

The validity and limitations of these assumptions will be discussed in § 4.

Let ε_0 be the starting energy of the electron, ε_m the maximum value of ε_0 and ρ the angle between the directions of the ion and electron flight (figure 1). According to relativistic collision dynamics one has the following relationship

$$\sin^2\rho = \frac{1-\varepsilon_0/\varepsilon_m}{1-\varepsilon_0/2m_ec^2} \tag{1}$$

assuming that the electron is initially at rest, m_e being the electron rest mass. ε_m is related to the ion's kinetic energy E, i.e. for non-relativistic cases

$$\varepsilon_m = \frac{4AE(1+E/2m_ic^2)}{(1+A)^2+2AE/m_ic^2} \tag{2}$$

with m_e and m_i the electron and ion masses respectively and $A = m_e/m_i$. Since $m_i \gg m_e$, if $E \ll m_ic^2$ (non-relativistic case) the following approximation may be used:

$$\varepsilon_m \simeq 4m_eE/m_i. \tag{3}$$

ε_m then depends only on the specific ion energy E/m_i.

The range R of electrons may be approximated by

$$R = K\varepsilon^\alpha \tag{4}$$

where ε is electron energy and K and α are adjustable parameters. According to the data compilation given by ICRU (1970) common values for K and α may be used for energies between about 200 and 10^5 eV. For water as the absorbing medium the best fit was obtained with $K = 4.18\times10^{-11}$ cm eV$^{-\alpha}$ and $\alpha = 1.70$.

By combining equations (1) and (4) one finds that the maximum distance x_0 perpendicular to the ion direction which an electron of starting energy ε_0 can travel is given by

$$x_0^2 = K^2\varepsilon_0^{2\alpha}\frac{1-\varepsilon_0/\varepsilon_m}{1+\varepsilon_0/2m_ec^2}. \tag{5}$$

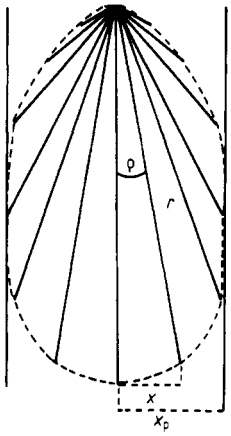

Figure 1. Schematic representation of angular distributions and ranges of electrons liberated by ion impact.

The penumbra radius x_p is the maximum of x_0 which can be found by differentiation of equation (5) with respect to ε_0. For the non-relativistic case ($\varepsilon_m \ll 2m_e c^2$) this leads to

$$x_p = K\left(\frac{2\alpha}{2\alpha+1}\right)^{\alpha}\left(\frac{1}{2\alpha+1}\right)^{1/2}\varepsilon_m^{\alpha}. \tag{6}$$

Inserting equation (3) one arrives at the numerical expression for water:

$$x_p = 6.16\times 10^{-2}(E/m_i)^{1.7} \tag{7}$$

where x_p is measured in μm, E in MeV and m_i in atomic mass units.

The general expression is not so simple. The penumbra radius may be found by inserting ε_p into equation (5) with

$$\varepsilon_p = \frac{1}{4aB}\{(2\alpha-1)B-(2\alpha+1)+[(2\alpha+1)^2(1+B)^2-8\alpha B(B+1)]^{1/2}\}$$

and

$$B = \varepsilon_m/2m_e c^2.$$

Numerical evaluation shows, however, that there is only a difference of about 5% between x_p according to equation (7) and the exactly calculated value up to ion specific energies of 1000 MeV u^{-1}. Equation (7) therefore appears to suffice for practical purposes within the energy range given.

Equation (4) may be used to determine the residual energy at a radial distance x from the centre:

$$\varepsilon(x,\varepsilon_0) = \varepsilon_0\left(1-\frac{x}{x_0}\right)^{1/\alpha} \tag{8}$$

where x_0 is the radial range of an electron with starting energy ε_0.

In order to obtain the total energy $\varepsilon(x)$ deposited between x and x_p one has to integrate over the contributions of all electrons whose radial ranges x_0 are larger than x. The distribution of starting energies is assumed to be (Butts and Katz 1967)

$$f(\varepsilon_0)\,\mathrm{d}\varepsilon_0 = C\frac{Z^{*2}}{\beta^2}\frac{1}{\varepsilon_0^2}\,\mathrm{d}\varepsilon_0. \tag{9}$$

C is a coefficient which depends only on the absorbing medium ($C = 8.5$ eV μm^{-1} for water (Butts and Katz 1967)), Z^* is the effective ion charge and β is its velocity relative to that of light in vacuum. With equation (9) one obtains

$$\varepsilon(x) = C\frac{Z^{*2}}{\beta^2}\int_{\varepsilon_{0_1}}^{\varepsilon_{0_2}}\frac{1}{\varepsilon_0}\left(1-\frac{x}{x_0}\right)^{1/\alpha}\mathrm{d}\varepsilon_0. \tag{10}$$

The differential energy loss $\mathrm{d}\varepsilon(x)/\mathrm{d}x$ is then

$$-\frac{\mathrm{d}\varepsilon(x)}{\mathrm{d}x} = C\frac{Z^{*2}}{\beta^2}\int_{\varepsilon_{0_1}}^{\varepsilon_{0_2}}\frac{1}{\alpha\varepsilon_0 x_0}\left(1-\frac{x}{x_0}\right)^{1/\alpha-1}\mathrm{d}\varepsilon_0. \tag{11}$$

The limits of integration ε_{01}, ε_{02} have to be determined as the roots of equation (5) for $x_0 = x$. This, as well as the integration of equation (11), can only be achieved

numerically. The computations are facilitated by the introduction of the following relative quantities:

$$\varepsilon_0' = \frac{\varepsilon_0}{\varepsilon_m} \qquad x' = \frac{x}{x_p} \qquad x_0' = \frac{x_0}{x_p}.$$

Equation (11) then takes the form

$$-\frac{d\varepsilon^{(x')}}{dx'} = C\frac{Z^{*2}}{\beta^2}\int_{\varepsilon_{0_1}'}^{\varepsilon_{0_2}'} \frac{1}{\alpha\varepsilon_0' x_0'}\left(1-\frac{x'}{x_0'}\right)^{1/\alpha-1} d\varepsilon_0'. \tag{11a}$$

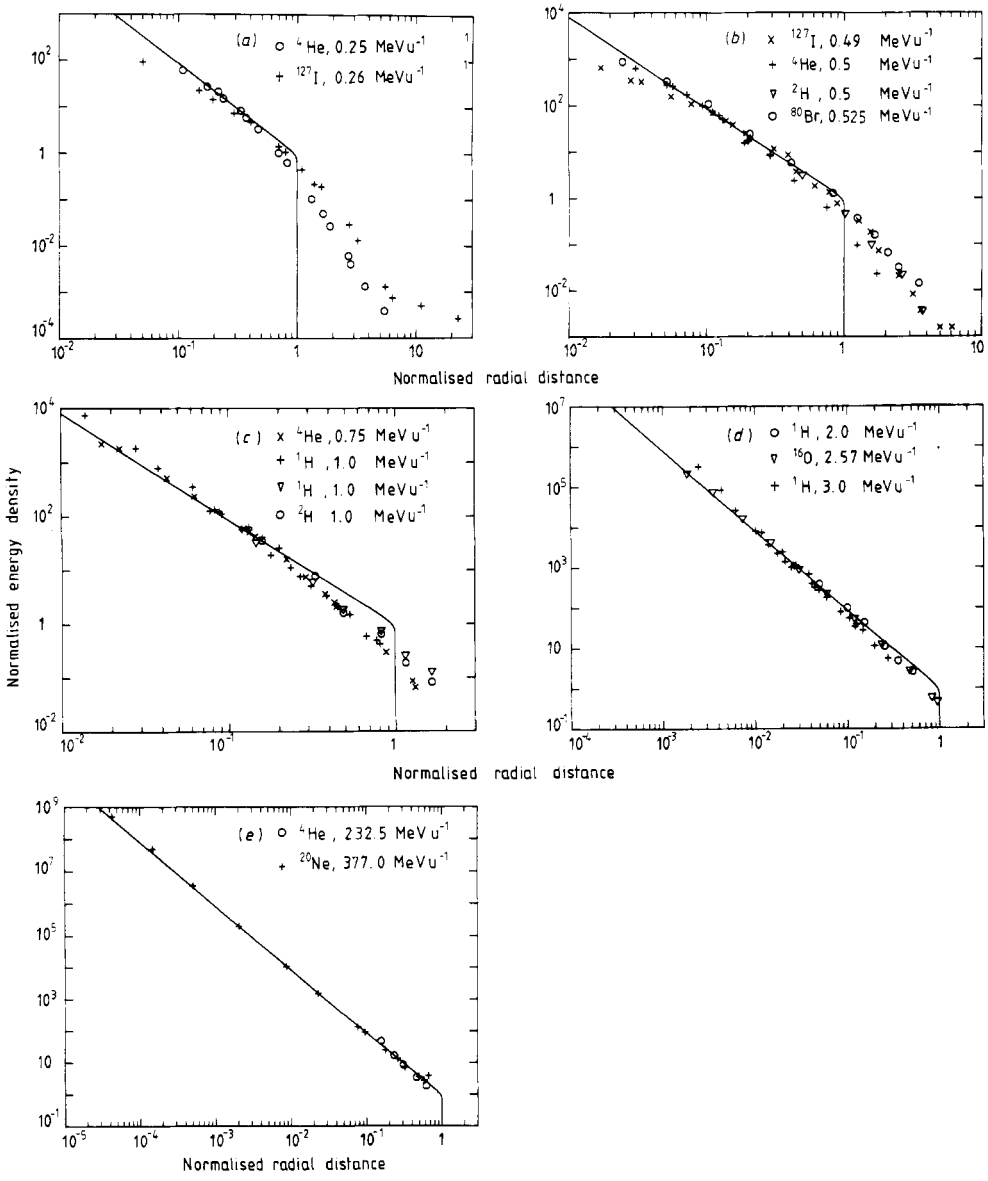

Figure 2. Comparison of experimental measurements of energy density with calculations. References are given in table 1. The full curves give the theoretical relationships according to the present model.

The energy density in relative units ρ'_e is accordingly

$$\rho'_e = \frac{1}{2\pi\rho_m x'} \frac{d\varepsilon(x')}{dx'} \tag{12}$$

where ρ_m is the density of the absorbing medium.

The results of the numerical calculation with water as the absorbing medium are shown in figure 2 in comparison with experimental measurements. In order to obtain the actual values the abscissa values have to be multiplied by x_p, and those of the ordinate by $Z^{*2}/\beta^2 x_p^2$. Figure 2 demonstrates that the energy density follows an $1/x^2$ dependence over many orders of magnitude. Very close to x_p there is a steeper decline but for practical purposes it may be assumed that there is a sudden cut-off at the penumbra radius. The functional dependence is given by

$$\rho'_e(x') = 0.78 \frac{Z^{*2}}{\rho_m \beta^2} x'^{-2} \text{ eV } \mu\text{m}^{-1}. \tag{13}$$

The actual energy density in Gy as a function of radial distance x measured in μm is then for water

$$\rho_e(x) = 1.25 \times 10^{-4} \frac{Z^{*2}}{\beta^2} x^{-2}. \tag{14}$$

3. Comparison with experimental results

Energy densities as a function of radial distance have been measured for a number of ions of various specific energies. These examples are listed in table 1 where the references are also given together with calculated values of Z^{*2}/β^2 and the penumbra radii according to the present model. Quantitative comparisons are made in figures 2(*a*)-(*e*). It is seen that the agreement is poor with ion specific energies below

Table 1. Experimental measurements of energy densities used for comparison with present results.

Ion	E/m_i (MeV u^{-1})	Z^{*2}/β^2	x_p† (μm)	Figure	Symbol in figure 3	Reference
^{1}H	1	463	0.061	2(*c*)	W	Wingate and Baum (1976)
^{1}H	3	156	0.39	2(*d*)	W	Wingate and Baum (1976)
^{1}H	1	463	0.061	2(*c*)	M	Menzel and Booz (1976)
^{1}H	2	233	0.20	2(*d*)	M	Menzel and Booz (1976)
^{2}H	0.5	901	0.02	2(*b*)	M	Menzel and Booz (1976)
^{2}H	1	463	0.061	2(*c*)	M	Menzel and Booz (1976)
^{4}He	0.25	5 241	0.006	2(*a*)	W	Wingate and Baum (1976)
^{4}He	0.5	3 183	0.02	2(*b*)	W	Wingate and Baum (1976)
^{4}He	0.75	2 279	0.037	2(*c*)	W	Wingate and Baum (1976)
^{4}He	232.5	11.1	655‡	2(*e*)	V6	Varma *et al* (1976)
^{16}O	2.57	9 460	0.30	2(*d*)	V7	Varma *et al* (1977)
^{20}Ne	377	203	1511‡	2(*e*)	VB	Varma and Baum (1980)
^{80}Br	0.525	114 000	0.02	2(*b*)	V8	Varma *et al* (1980)
^{127}I	0.26	179 000	0.006	2(*a*)	B	Baum *et al* (1974)
^{127}I	0.49	169 000	0.018	2(*b*)	B	Baum *et al* (1974)

† Penumbra extension calculated according to equation (7), except where otherwise indicated.
‡ Calculated relativistically as described in the text.

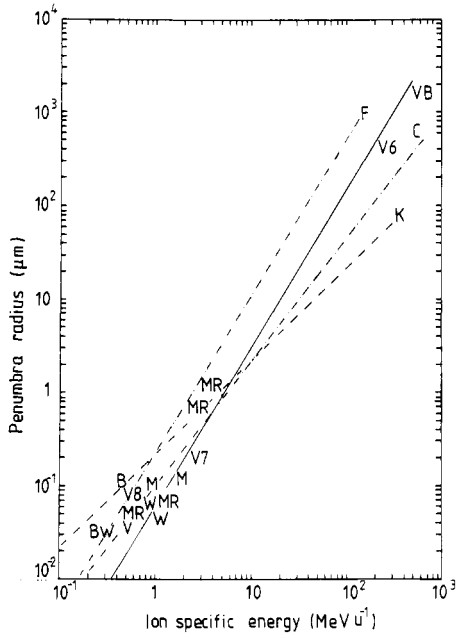

Figure 3. Estimates of penumbra radii from experimental measurements compared with the calculations of different authors: C, Chatterjee *et al* (1973); K, Butts and Katz (1967); F, Fain *et al* (1974); W, Wingate and Baum (1976); M, Menzel and Booz (1976); V6, Varma *et al* (1976); V7, Varma *et al* (1977); V8, Varma *et al* (1980); VB, Varma and Baum (1980); B, Baum *et al* (1974); MR, Mills and Rossi (1980); full line, this paper. See table 1 for details.

2 MeV u^{-1}. This is not surprising since the approximations used are highly questionable with low energies (see below). It has also to be taken into account that the measured radial distributions are influenced by electron diffusion which is particularly important for small distances. Acceptable agreement between theory and experiment is found for higher specific energies, even for relativistic heavy ions. The 1 MeV proton and deuteron experimental data show a clear deviation from the $1/x^2$ dependence. It is not clear whether this may be due to an experimental artefact caused by the very low values of energy densities which had to be measured.

As previously mentioned, the maximum extension of the track, the penumbra radius, is a critical parameter for the interpretation of the action of very heavy ions. It is here that the different models differ most extensively. Experimental measurements can obviously only supply lower limits but they may serve as a feasability check. In figure 3 estimates taken from various sources are compared with calculated results. It is seen that the present model works quite well for specific ion energies greater than 1 MeV u^{-1} while it fails below this limit. It appears that penumbra radii cannot be described by a unique power function of specific energy over the whole region from 0.25 to several hundreds of MeV u^{-1} and that a different expression is required for low specific energies.

4. Discussion

The simplifying assumptions made have to be critically discussed. The electrons are assumed to be unbound so that the interaction processes can be treated using collision dynamics. If binding is taken into account the unique relationship between ejection

angle and energy (equation (1)) breaks down. This will be particularly important for small electron energies and certainly contributes to the fact that our model does not fit the experimental data at low specific ion energies. With higher electron energies the energy–angle distributions display kinematic peaks (Wilson and Torburen 1981) which coincide with the classically derived values.

The maximum energy transfer to bound electrons may be considerably larger than to free ones. This is again particularly important for low energies.

Electron scattering is another problem. There appears to be no way of treating this analytically; the only feasible approach is a Monte Carlo simulation. It is therefore not surprising that Paretzke's calculations show a very good agreement with the measurements of Varma *et al* (1980). For heavier ions, experimental cross sections which are required for Monte Carlo calculations are not yet available. Another disadvantage is that each ion and each energy has to be treated by a separate calculation which is time consuming and costly.

Scattering is implicitly incorporated in our model by using 'practical' electron ranges. The assumption of a continuous energy loss along a straight line is certainly not exactly justified but this does not play an essential role since energy deposition is treated in an integral way so that local variations are averaged. For low-energy electrons scattering may be very important leading to higher penumbra extensions then predicted by the straight-line approximation.

Ejection cross sections are known only for lighter ions. We assume that the $1/\varepsilon^2$ relation holds if approximately scaled by Z^{*2}/β^2. For 1 MeV protons the inverse square dependency holds over a wide range between 200 and 2000 eV (Wilson and Torburen 1981) but this may be questionable for heavier ions and higher energies. So long as sufficient experimental data are not available the approximation made appears to be the only approach. Comparison with experimental track structure data shows a good fit for energy densities as a function of radial distance. This is not necessarily a proof of the validity of the assumptions since integral calculations like those presented here are remarkably insensitive to variations of the input parameters, as pointed out by Varma *et al* (1976). Calculated penumbra radii are compatible with experiments for ion specific energies above about 1 MeV u^{-1}.

In the lower region they are systematically underestimated. This is not surprising, however, since here the assumptions made are no longer tenable.

The first model to calculate energy densities around an ion track was introduced by Butts and Katz (1967). They assumed that all electrons are ejected perpendicularly to the ion path and that they have constant energy loss irrespective of their energy. This is clearly at variance with experimental results (see, for example, Wilson and Torburen 1981) and commonly accepted stopping-power theory. Chatterjee's model (Chatterjee *et al* 1973, Chatterjee and Schaefer 1976) relies on the equipartition principle, leading to a distinction between a track 'core' and the penumbra with a discontinuity between them. The penumbra extension is only given by a semi-empirical formula. Baum (1970) used a classical approach similar to ours and demonstrated its applicability for calculations of energy- and range-restricted LET. The model by Fain *et al* (1974) also bears some resemblance to the present one. These authors used classical collision dynamics for the angular distribution of electrons but used binary encounter theory (Gryziński 1965) for the energy distribution. The relationship obtained for the energy density as a function of radial distance is virtually identical to our equation (14) which demonstrates that the much simpler classical approach is sufficient. Penumbra radii were not explicitly derived but only stated as a mathematical

expression, presumably semi-empirically obtained. Hansen and Olsen (1984) use essentially the approach of Fain *et al* with some refinements. The main advantage of the treatment in our work is that penumbra radii are explicitly derived and appear to be compatible with experimental values, even for relativistic heavy ions. In conclusion, it is hoped that the model described may be useful in its simplicity for the quantitative interpretation of biological heavy-ion data.

Acknowledgments

JK would like to thank the Deutsche Forschungsgemeinschaft for a travel grant and Dr A Chatterjee for fruitful discussions. This study was partly supported by Gesellschaft für Schwerionenforschung (GSI), Darmstadt.

Résumé

Modélisation de la trace des ions reposant sur la théorie classique des collisions.

Les auteurs calculent le dépôt d'énergie le long des traces d'ions en fonction de la distance radiale, en utilisant la théorie classique des collisions et des relations empiriques entre le parcours et l'énergie des électrons. Ces calculs montrent que l'énergie massique (c'est-à-dire l'énergie déposée par unité de masse) varie comme l'inverse du carré de la distance au centre de la trace. L'extension maximale de la trace, appelée 'rayon de la pénombre', est une fonction puissance de l'énergie cinétique de l'ion, divisée par sa masse. Une comparaison avec les données expérimentales démontre la validité du modèle pour des énergies caractéristiques des ions supérieures à 1 MeV u^{-1}.

Zusammenfassung

Ein Modell der Bahnstruktur schwerer Ionen auf der Grundcase der klassichen Stossdynamik.

Es wird die Energiedeposition durch beschleunigte Ionen als Funktion der radialen Bahnausdehnung auf der Basis der relativistischen Stoßmechanik und unter Zuhilfenahme empirischer Energie-Reichweite-Beziehungen für Elektronen berechnet. Die Ergebnisse zeigen, daß die Energiedichte (d.h. deponierte Energie pro Massenelement) mit dem Quadrat des Abstandes vom Bahnzentrum abnimmt. Die maximale Ausdehnung, der 'Pänumbra-Radius', ist eine Potenzfunktion der spezifischen Ionenenergie (d.h. kinetische Energie dividiert durch Ionenmasse). Ein Vergleich mit experimentellen Messungen zeigt, daß dieses Modell für spezifische Ionenenergien über 1 MeV u^{-1} eine gute Annäherung darstellt.

References

Baum J W 1970 *Proc. 2nd Symp. Microdosimetry* (*Brussels*) ed H G Ebert (EUR 4452 d-f-e) pp 653-66
Baum J W, Varma M N, Wingate C L, Paretzke H G and Kuehner A V 1974 *Proc. 4th Symp. Microdosimetry* (*Luxembourg*) ed J Booz, H G Ebert, R Eickel and A Waker (EUR 5122 d-e-f) pp 93-112
Blakely E A, Ngo F Q H, Curtis S B and Tobias C A 1984 *Adv. Radiat. Biol.* **11** 295-390
Brenner D J and Zaider M 1984 *Radiat. Res.* **98** 14-25
Butts J J and Katz R 1967 *Radiat. Res.* **30** 855-71
Chatterjee A, Maccabee H D and Tobias C A 1973 *Radiat. Res.* **54** 479-94
Chatterjee A and Schaefer H J 1976 *Radiat. Environ. Biophys.* **13** 215-27
Fain J, Monin M and Montret M 1974 *Proc. 4th Symp. Microdosimetry* (*Luxembourg*) ed J Booz, H G Ebert, R Eickel and A Waker (EUR 5122 d-e-f) pp 169-88
Gryziński M 1965 *Phys. Rev.* **138** A336-58
Hansen J W and Olsen K J 1984 *Radiat. Res.* **97** 1-5
ICRU 1970 *Linear Energy Transfer, Report No 16* (Washington, DC: ICRU)
Kiefer J 1985 *Int. J. Radiat. Biol.* **48** 873-92

Menzel H G and Booz J 1976 *Proc. 5th Symp. Microdosimetry* (*Luxembourg*) ed J Booz, H G Ebert and B G R Smith (EUR 5452 d-e-f) pp 61–74

Mills R E and Rossi H H 1980 *Radiat. Res.* **84** 434–43

Paretzke H G 1974 *Proc. 4th Symp. Microdosimetry* (*Luxembourg*) ed J Booz, H G Ebert, R Eickel and A Waker (EUR 5122 d-e-f) pp 141–68

—— 1980 *Advances in Radiation Protection and Dosimetry in Medicine* ed R H Thomas and V Perez-Mendes (New York: Plenum) pp 51–73

Varma M N and Baum J W 1980 *Radiat. Res.* **81** 355–63

Varma M N Baum J W and Kuehner A V 1977 *Radiat. Res.* **70** 511–8

—— 1980 *Phys. Med. Biol.* **25** 651–6

Varma M N Paretzke H G, Baum J W, Lyman J T and Howard J 1976 *Proc. 5th Symp. Microdosimetry* (*Luxembourg*) ed J Booz, H G Ebert and B G R Smith (EUR 5452 d-e-f) pp 75–95

Wilson W E and Paretzke H G 1981 *Radiat. Res.* **87** 521–37

Wilson W E and Toburen L H 1981 *Proc. 7th Symp. Microdosimetry* (*Brussels and Luxembourg*) ed J Booz, H G Ebert and H D Hartfiel (Harwood) pp 435–48

Wingate C L and Baum J W 1976 *Radiat. Res.* **65** 1–19

Zaider M, Brenner D J and Wilson W E 1983 *Radiat. Res.* **95** 231–47